

Fig. 3 Buckling of toroidal segments under external lateral pressure—positive gaussian curvature.

#### Analysis and Results

Stein and McElman<sup>4</sup> have given a closed-form solution for the buckling of simply supported toroidal segments symmetric about the equator. Specifically, the critical pressure is

$$p_{cr} = k\pi^2 D/r_t l^2$$

where  $l$  is the length of the shell,  $D$  the flexural stiffness,  $r_t$  the throat radius, and  $k$  is evaluated by minimizing the expression

$$k = [(1 + \beta^2)^4 + (12Z^2/\pi^4)(1 - \alpha\beta^2)^2]/B \quad (1)$$

with respect to  $\beta$  for given  $Z$  and  $\alpha$ , where  $\alpha = r_t/a$ ,  $\beta = nl/(\pi r_t)$ ,  $a$  is the radius of curvature of the meridian, and

$$Z = (l^2/r_t t)(1 - \mu^2)^{1/2}$$

$$B = \beta^2(1 + \beta^2)^2 \quad \text{for lateral pressure}$$

$$B = 0.5(1 + 2\beta^2 - \alpha\beta^2)(1 + \beta^2)^2 \quad \text{for hydrostatic pressure}$$

Abel and Billington<sup>3</sup> suggest that Eq. (1) be applied to cooling towers by considering only the top part of the tower for which the throat is the midheight. As a check of the applicability of this procedure, the finite-element method was used to analyze the toroidal segment shown in Fig. 1.

#### Conclusions

The Stein and McElman<sup>4</sup> theory is limited to shallow shell approximations and to buckling near the equator of a toroidal shell segment. For the lateral pressure case and particular shell geometry, it was found that a more accurate finite-element shell buckling solution agree approximately with the Stein and McElman<sup>4</sup> predictions only for the positive curvature shell. Experimental results from Veronda<sup>5</sup> were in good agreement with the finite-element solution and were far away from predicted values obtained from the Stein and McElman<sup>4</sup> design curves. It appears that the assumptions used by Stein and McElman are very restrictive and must be checked for each specific design case by using a more accurate shell stability solution.

#### References

- <sup>1</sup> Column Research Committee of Japan, ed., *Handbook of Structural Stability*, Corona Publishing, Tokyo, Japan, 1972.
- <sup>2</sup> *Buckling of Thin Walled Doubly Curved Shells*, NASA SP-8032, Aug. 1969.
- <sup>3</sup> Abel, J. F. and Billington, D. P., "Stability Analysis of Cooling Towers: A Review of Current Methods," *Proceedings of the IASS Symposium of Shell Structures and Climatic Influences*, 1972, pp. 455-465.

<sup>4</sup> Stein, M. and McElman, J. A., "Buckling of Segments of Toroidal Shells," *AIAA Journal*, Vol. 3, No. 9, Sept. 1965, pp. 1704-1709.

<sup>5</sup> Veronda, D., "Stability of Hyperboloidal Shells: An Experimental and Analytical Investigation," Ph.D. dissertation, 1973, Univ. of Southern California, Los Angeles, Calif.

<sup>6</sup> Lashkari, M., Weingarten, V. I., and Margolis, D., "Effect of Lateral Pressure on the Natural Frequencies of Hyperboloidal Shells of Revolution," *Journal of Engineering Mechanics Division, ASCE*, Vol. 98, No. EM5, Oct. 1972, pp. 1017-1031.

## CO<sub>2</sub> Laser Radiation Absorption in SF<sub>6</sub>-Air Mixtures

JOHN D. ANDERSON JR.,\* JERRY L. WAGNER,† AND  
JOSEPH KNOTT†  
Naval Ordnance Laboratory, Silver Spring, Md.

#### I. Introduction

GASEOUS sulfur hexafluoride (SF<sub>6</sub>) is a strong absorber of radiation at 10.6  $\mu$ . This wavelength also corresponds to the output from common CO<sub>2</sub> lasers. As a result of this resonance phenomena, SF<sub>6</sub> has found applications in Q switching and mode locking CO<sub>2</sub> gas lasers, and has been useful in other aspects of laser physics as itemized by Steinfeld et al.<sup>1</sup> In turn, these applications have prompted fundamental measurements of SF<sub>6</sub> infrared absorption coefficients,<sup>2-8</sup> and encouraged studies of its saturation and self-induced transparency effects.<sup>5-9</sup>

The addition of SF<sub>6</sub> to air, and the subsequent laser radiation absorption in such SF<sub>6</sub>-air mixtures, has potential applications in aerodynamics for tailoring flows for useful purposes. Several examples are discussed in Ref. 10. Moreover, it has potential as a unique energy conversion mechanism, such as in photon engines.<sup>11</sup> The purpose of this Note is to present physical data on the 10.6  $\mu$  radiation absorption and saturation properties of SF<sub>6</sub>-air mixtures; these data are needed for future aerodynamic applications.

#### II. Absorption Coefficient

The molecular properties of SF<sub>6</sub> are summarized in Refs. 10 and 12. The absorption of CO<sub>2</sub> laser radiation by SF<sub>6</sub> occurs, in part, between the ground state and the first excited level of the  $\nu_3$  vibrational mode. Hot band absorption also occurs from the first excited level of the  $\nu_6$  mode to the first combined ( $\nu_3 + \nu_6$ ) level. Moreover, the present results, as well as those of Ref. 13, imply that additional hot band absorption from other low-lying vibrational levels must be considered. For each of these vibrational transitions, the 10.6  $\mu$  laser radiation is absorbed by a large number of overlapping vibration-rotation lines; hence, the pressure broadened absorption coefficient for each vibrational transition is<sup>14</sup>

Presented as Paper 73-262 at the AIAA 11th Aerospace Sciences Meeting, Washington, D.C., January 10-12, 1973; submitted January 31, 1973; revision received June 21, 1973. This work was supported in part by the Naval Air Systems Command under Air Task A310310A/292A/2R02102-001, and by the Naval Ordnance Laboratory Independent Research Funds.

Index categories: Radiation and Radiative Heat Transfer; Atomic, Molecular, and Plasma Properties.

\* Chief, Hypersonics Group; presently Professor and Chairman, Aerospace Engineering Department, University of Maryland, College Park, Md. Member AIAA.

† Aerospace Engineer, Hypersonics Group.

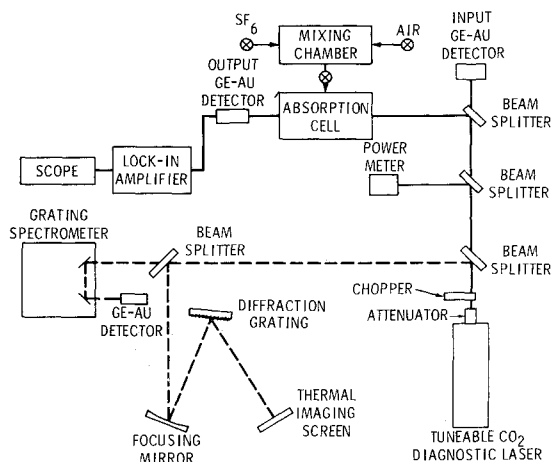


Fig. 1 Schematic diagram of absorption cell apparatus.

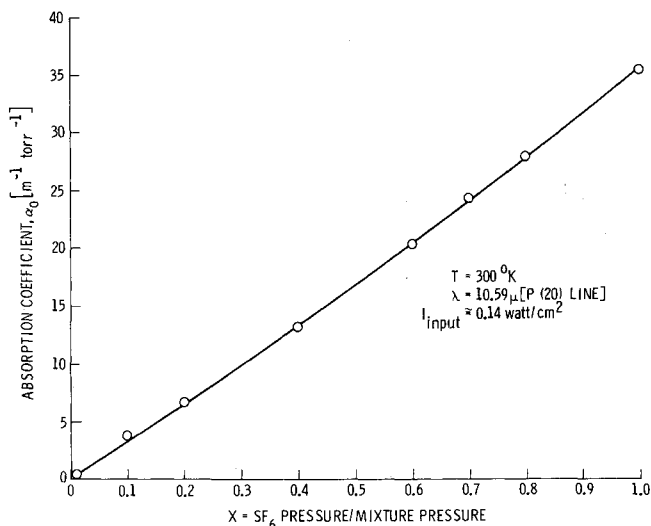
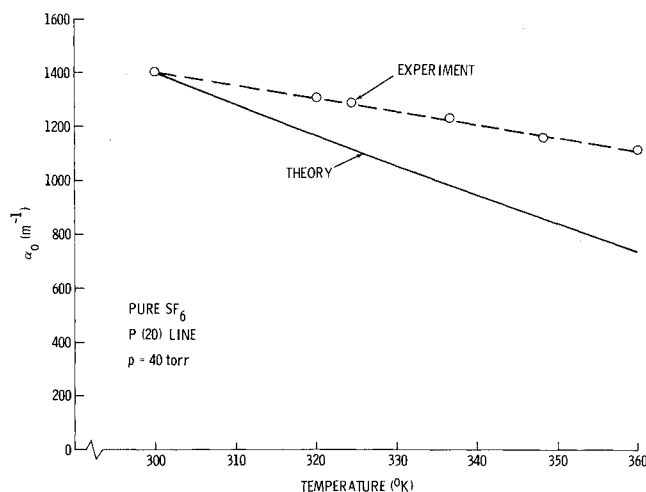
$$\alpha_0(\nu) = \frac{\lambda^2}{4\pi^2 \Delta\nu} \sum_j A_{21j} \left( N_{1j} - \frac{g_1}{g_2} N_{2j+1} \right) \left[ 4 \left( \frac{\nu - \nu_j}{\Delta\nu} \right)^2 + 1 \right]^{-1}$$

where  $N_{2j+1}$  and  $N_{1j}$  are the populations of the upper and lower vibration-rotation energy levels, respectively, and  $\lambda$ ,  $\Delta\nu$ ,  $A_{21j}$ ,  $g_1$ , and  $g_2$  are the wavelength, line width, Einstein coefficient, and statistical weights, respectively. Replacing the sum by an integral, the absorption coefficient for  $\text{CO}_2$  laser radiation due to a given vibrational transition in  $\text{SF}_6$  becomes

$$\alpha_0 = A_{21} \phi_1 [N_1 - (g_1/g_2) N_2]$$

where  $\phi_1$  is a function of temperature and all other subscripts refer to the respective vibrational levels. From this equation, the effect of a large number of overlapping lines is to cause  $\alpha_0$  to vary linearly with pressure. This is in contrast to the case of a single pressure broadened line, where  $\alpha_0$  at line center is independent of pressure.

The present results extend previous measurements<sup>2-8</sup> of the  $10.6\mu$  absorption coefficient for pure  $\text{SF}_6$  to higher pressures and temperatures. Moreover, the present measurements give the first results for  $\alpha_0$  in  $\text{SF}_6$ -air mixtures of interest in aerodynamic applications. A schematic of the experimental setup for the present absorption coefficient measurements is shown in Fig. 1.

Fig. 2 Variation of absorption coefficient with  $\text{SF}_6$  mole fraction in  $\text{SF}_6$ -air mixtures.Fig. 3 Temperature variation of  $\text{SF}_6$  absorption coefficient.

A portion of the chopped output beam from a stable tuneable  $\text{CO}_2$  laser passes through a 5-mm-long absorption cell, which contains a regulated  $\text{SF}_6$ -air mixture at desired pressure and temperature. Five basic laser measurements are monitored: input intensity to the absorption cell, output intensity from the absorption cell, average power, wavelength, and mode shape. The apparatus and experimental procedure are described in Ref. 10. The data obtained for a large range of mixture pressure and mole fractions, as well as for  $\text{CO}_2$  laser wavelengths from the  $P(10)$  to  $P(32)$  transitions, are also given in Ref. 10. These data show that  $\alpha_0$  is indeed a linear function of pressure for all wavelengths and mole fractions considered. Some results are shown in Fig. 2, where the absorption coefficient in units of  $(\text{m}^{-1} \text{ torr}^{-1})$  is given as a function of the mole fraction of  $\text{SF}_6$ . The linear variation shown in this figure clearly demonstrates that  $\alpha_0$  is dependent on the number density of  $\text{SF}_6$ , and is independent of the number density of air. Therefore, the pressure broadening cross sections for  $\text{SF}_6$ -air collisions must be of the same order as those for  $\text{SF}_6$ - $\text{SF}_6$  collisions. Moreover, for pure  $\text{SF}_6$ , the present data indicate that  $\alpha_0 = 35.4 \text{ m}^{-1} \text{ torr}^{-1}$ ; this agrees very well with the value of  $35.7 \text{ m}^{-1} \text{ torr}^{-1}$  obtained from the data of Ref. 8.

The variation of  $\alpha_0$  over a moderate range of  $T$  is shown in Fig. 3. The observed reduction of  $\alpha_0$  with increasing  $T$  is not as large as expected on theoretical grounds including just the ground state and the first hot band absorptions.<sup>10</sup> This implies that additional hot band absorptions may contribute to  $\alpha_0$ , even at room temperature.

### III. Saturation Effects

If the laser beam is intense enough and the gas density is low enough, molecular excitation due to photon absorption can dominate the de-excitation due to molecular collisions, causing the ground state population to be depleted and the excited levels to become overpopulated. This vibrational nonequilibrium causes  $\alpha$  to become a function of the incident laser intensity,  $I_{\text{in}}$ , i.e.,  $\alpha$  is influenced by saturation effects.

Saturation intensities in pure  $\text{SF}_6$  have been measured previously at low pressures.<sup>6,7</sup> However, no results (experimental or theoretical) at near-atmospheric pressures in  $\text{SF}_6$ -air mixtures of aerodynamic interest have been available. Such results are given in Fig. 4; here,  $\alpha$  is given as a function of  $I_{\text{in}}$  for a 10%  $\text{SF}_6$ -90% air mixture at pressures corresponding to standard altitudes of sea level, 10,000 ft and 20,000 ft. These are theoretical results obtained from the kinetic model and nonequilibrium analysis described in Ref. 10. A constant temperature gas is assumed, hence isolating the purely nonequilibrium effects from

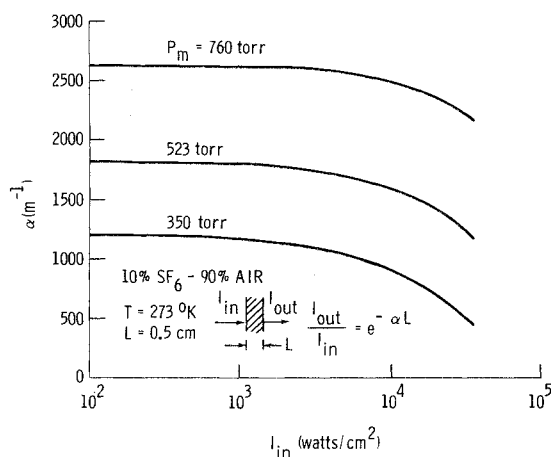


Fig. 4 Predicted saturation effects in a constant temperature  $\text{SF}_6$ -air mixture at near-atmospheric pressures.

the influence of bulk heating.<sup>10</sup> The vibrational relaxation times used in this analysis are from Ref. 1, where  $p\tau_{\text{SF}_6-\text{SF}_6} = 122 \mu\text{sec-torr}$ , and  $p\tau_{\text{SF}_6-\text{N}_2} = 103 \mu\text{sec-torr}$ . This latter value is adopted for  $p\tau_{\text{SF}_6-\text{air}}$ . The results shown in Fig. 4 suggest that saturation effects for a typical  $\text{SF}_6$ -air mixture at near-atmospheric pressure are not important until  $I_{\text{in}}$  exceeds  $10^4 \text{ w/cm}^2$ .

#### IV. Conclusions

From the results given in this Note, and from the extensive data shown in Refs. 10 and 12 (on which this Note is based), the following conclusions are made.

- 1) Pure  $\text{SF}_6$  is a powerful absorber of  $10.6\mu$  radiation. For example, the small-signal absorption coefficient,  $\alpha_0$  for  $\text{SF}_6$  is on the order of  $3540 \text{ m}^{-1}$  at  $p = 100 \text{ torr}$ .
- 2)  $\text{SF}_6$ -air mixtures are also strong absorbers of  $10.6\mu$  radiation. For example,  $\alpha_0 = 2740 \text{ m}^{-1}$  in a 10%  $\text{SF}_6$ -90% air mixture at 1 atm.
- 3) The experimental variation of  $\alpha_0$  with  $p$  is linear. This is consistent with the theoretical prediction for absorption due to a large number of closely spaced overlapping lines.
- 4) Comparison between experimental data and theory imply that additional (and as yet unidentified) hot band transitions are contributing to  $\text{SF}_6$  absorption at room temperature and above.
- 5) At pressures near atmospheric, the onset of saturation for a 10%  $\text{SF}_6$ -90% air mixture occurs above intensities of  $10^4 \text{ w/cm}^2$ .

#### References

- 1 Steinfeld, J. I., Burak, I., Sutton, D. G., and Nowak, A. V., "Infrared Double Resonance in Sulfur Hexafluoride," *Journal of Chemical Physics*, Vol. 52, No. 10, May 1970, pp. 5421-5434.
- 2 Shimizu, F., "Absorption of  $\text{CO}_2$  Laser Lines by  $\text{SF}_6$ ," *Applied Physics Letters*, Vol. 14, No. 12, June 1969, pp. 378-380.
- 3 Hinkley, E. D., "High-Resolution Infrared Spectroscopy with a Tunable Diode Laser," *Applied Physics Letters*, Vol. 16, No. 9, May 1970, pp. 351-354.
- 4 Abrams, R. L. and Dienes, A., "Cross Saturation of  $10.6\mu$  Signals in  $\text{SF}_6$ ," *Applied Physics Letters*, Vol. 14, No. 8, April 1969, pp. 237-240.
- 5 Oppenheim, U. P. and Melman, P., "Excited-State Absorption of  $\text{SF}_6$  at  $936.8 \text{ cm}^{-1}$ ," *IEEE Journal of Quantum Electronics*, Vol. QE-7, No. 8, Aug. 1971, pp. 426-427.
- 6 Brunet, H., "Saturation of Infrared Absorption in  $\text{SF}_6$ ," *IEEE Journal of Quantum Electronics*, Vol. QE-6, No. 11, Nov. 1970, pp. 678-684.
- 7 Burak, I., Steinfeld, J. I., and Sutton, D. G., "Infrared Saturation in Sulfur Hexafluoride," *Journal of Quantitative Spectroscopy and Radiative Transfer*, Vol. 9, No. 7, 1969 pp. 959-980.
- 8 Rhodes, C. K. and Szoke, A., "Transmission of Coherent Optical Pulses in Gaseous  $\text{SF}_6$ ," *Physical Review*, Vol. 184, No. 1, Aug. 1969, pp. 25-37.

<sup>9</sup> Patel, C. K. N. and Slusher, R. E., "Self-Induced Transparency in Gases," *Physical Review Letters*, Vol. 19, No. 18, Oct. 1967, pp. 1019-1022.

<sup>10</sup> Anderson, J. D., Wagner, J. L., and Knott, J., " $\text{CO}_2$  Laser Radiation Absorption in  $\text{SF}_6$ -Air Boundary Layers," NOLTR 72-172, Aug. 1972, Naval Ordnance Lab., White Oak, Md.

<sup>11</sup> Hertzberg, A. et al., "Photon Generators and Engines for Laser Power Transmission," *AIAA Journal*, Vol. 10, No. 4, April 1972, pp. 394-400.

<sup>12</sup> Anderson, J. D., Jr., Wagner, J. L., and Knott, J., " $\text{CO}_2$  Laser Radiation Absorption in  $\text{SF}_6$ -Air Boundary Layers," AIAA Paper 73-262, Washington, D.C., 1973.

<sup>13</sup> Armstrong, J. J. and Gaddy, O. L., "Saturation Behavior of  $\text{SF}_6$  at High Pressure and Laser Intensity," *IEEE Journal of Quantum Electronics*, Vol. QE-8, No. 10, Oct. 1972, pp. 797-802.

<sup>14</sup> Lengyel, B. A., *Lasers*, 2nd ed., Wiley-Interscience, New York, 1971, pp. 12-25.

## Reattachment of a Separated Boundary Layer to a Convex Surface

JAMES L. AMICK\* AND TARIQ MASOUD†  
The University of Michigan, Ann Arbor, Mich.

**E**XPERIMENTS on simplified models of the interaction between a transverse two-dimensional jet and an enveloping supersonic flow have been conducted at the Gas Dynamics Labs. of The Univ. of Michigan.<sup>1</sup> One of the simplified models consisted of a flat plate upon which was mounted a solid obstacle representing the jet (see Fig. 1). The shape chosen for this obstacle was a cylinder of semicircular cross section, the flat side of which was placed against the flat plate, with the cylinder axis perpendicular to the flow direction. The forward part of this circular cylinder thus represents a portion of the dividing stream surface between an imagined two-dimensional transverse jet and the main airstream. The flow ahead of this simulated jet behaves very much like that ahead of a real jet, in that it separates from the plate at some distance ahead of the jet, and then reattaches to the convex (jet) surface while undergoing a strong interaction shock. The flow pattern is also quite similar to that ahead of a forward-facing step, with the important difference that reattachment is not constrained to occur at a fixed point (the corner of the step). This Note describes experimental determinations of the location of reattachment on the curved surface, and correlation with a simple theory.

The tests were conducted at Mach number 3.9 and Reynolds number 120,000 per inch in the 8- by 13-in. supersonic wind tunnel of The Univ. of Michigan, on the two-dimensional model shown in cross section in Fig. 1. The semicircular cylinder had a diameter of 1 in. and a span of 3 in. The flat plate on which it

Received December 13, 1972; revision received March 16, 1973. This work was sponsored by the Naval Ordnance Systems Command, under Subcontract 181462 with the Applied Physics Laboratory of the Johns Hopkins University. The authors are indebted to P. O. Hays, Research Engineer, The University of Michigan, who conducted the turbulent boundary-layer tests.

Index categories: Boundary Layers and Convective Heat Transfer—Laminar; Boundary Layers and Convective Heat Transfer—Turbulent; Supersonic Flow.

\* Research Engineer, Department of Aerospace Engineering; now consultant. Member AIAA.

† Graduate student, Department of Aerospace Engineering; now Senior Research Officer, Defence Science Organization, Chaklala, Pakistan.